Korean J. Chem. Eng., **26**(6), 1453-1460 (2009)
DOI: 10.2478/s11814-009-0252-1

Combined run-to-run and LQG control of a 12-inch RTP equipment

Wangyun Won*, Woohyun Yun*, Sang Hyun Ji, Byung-Cheol Na**, and Kwang Soon Lee*,†**

*Department of Chemical and Biomolecular Engineering, Sogang University,
1-Shinsoodong, Mapogu, Seoul 121-742, Korea
**KORNIC Systems Co. Ltd., Jungri, Dongtanmyun, Hwasung, Gyeonggi-do 445-813, Korea
(*Received 8 February 2009 • accepted 5 April 2009*)

Abstract−A combined run-to-run (R2R) and LQG control method has been proposed for rapid thermal processing (RTP) equipment for run-wise improvement and real-time multivariable control of the temperature uniformity over the wafer surface. The standard LQG objective was modified to include a quadratic penalty term for input deviation from bias values which are updated by an R2R control law. The proposed method has been applied to commercial 12-inch rotating RTP equipment with four pyrometers and ten circular groups of tungsten-halogen lamps for measurements and manipulation of wafer temperatures. The performance of LQG control was evaluated under wafer rotation and found to show quite accurate tracking. For evaluation of the combined control technique, a wafer with seven thermocouples (TC's) attached along the radial direction has been employed for the TC measurements to be used for R2R control, whereas the pyrometer measurements are fed back for real-time LQG control. It was observed that the temperature uniformity is improved as the run number increases.

Key words: Rapid Thermal Processing, LQG Control, Run-to-run Control, QILC

INTRODUCTION

Due to low thermal budget, rapid thermal processing (RTP) is widely employed for various semiconductor fabrications such as annealing, oxidation, nitridation, etc., and has become an indispensable process in semiconductor industries. The most important operation requirement in RTP is to maintain a high degree of temperature uniformity across the wafer surface.

Most present commercial RTP equipment employs tungsten-halogen (TH) lamps for wafer heating and pyrometers for temperature measurement, which form a closed-loop for real-time temperature control. The shape and arrangement of the lamps are usually protected by patents, hence differing from system to system. The number of pyrometer installations depends on systems but is typically limited by six to seven in 12-inch RTP equipment due to the space availability and cost. To assess the temperature uniformity, therefore, rapid thermal oxidation (RTO) or rapid thermal annealing (RTA) of a bare or doped wafer is conducted additionally and oxide layer thickness (OT) or resistivity (RS) distribution is measured. When the uniformity does not meet the prescribed specifications, the power ratio of lamp groups and/or set points of the pyrometer temperatures (pyro-temperatures) or other handles are adjusted either heuristically or systematically. In this way, commercial RTP systems are run under two feedback loops, an inner loop for real-time temperature control and an outer loop for run-wise betterment of the temperature uniformity.

For real-time control of RTP equipment, there have been continuous studies as has been reviewed in Edgar et al. [1] Various control methods have been attempted including decoupling control [2], proportional-double integral-derivative control [3], iterative learning control [4-8], adaptive control [9], internal model control [10], LQG control [11], etc. Although PID control is still practiced in some commercial systems, it seems that model-based multivariable control, whatever the law is, has become an indispensable technique to meet the ever tightening uniformity specifications in the present 12-inch and future RTP equipment. For run-wise uniformity improvement of the OT or RS map, however, there have been few published researches, although the step is necessary in any case for possible operation in a production line.

This paper describes an integrated multivariable control technique developed for a commercial 12-inch rotating RTP equipment. The control system is designed to conduct run-wise uniformity improvement together with real-time LQG control. At the core of the control system is an LQG controller modified from the standard formulation to include a quadratic penalty term on input deviation from given bias values. The input bias affects the temperature distribution and thus was designed to be updated run-wise by using a run-to-run (R2R) control method. The LQG performance largely depends on the quality of the process model. To cope with this, a procedure to determine a MIMO balanced state space model through multiple SIMO (single-input multiple-output) identification experiments has been devised, too. Experimental investigation has been conducted with a rotating wafer with only pyrometer measurements and also a non-rotating thermocouple-attached wafer (TC-wafer) for LQG control and for combined R2R and LQG control, respectively.

PROCESS DESCRIPTION

Fig. 1 is a photograph of the Korona^{TM}1200*Plus* system from KORNIC Systems Co., Ltd., Korea for which the control study has been conducted. It has two identical RTP chambers for 12-inch wafers rotating at 150 rpm-max. The inner surface of the chamber wall is gold-plated for maximum reflectivity and the wall temperature is regulated by cooling water circulating inside the wall. The equip-

†To whom correspondence should be addressed.
E-mail: kslee@sogang.ac.kr

Fig. 1. Photograph of Korona^{TM}1200*Plus* system.

ment has 220 bulb-type 0.7 kw-max TH lamps arranged in ten concentric circles for wafer heating. The power of each lamp circle can be manipulated individually. Under normal operation with wafer rotation, temperatures are measured with four pyrometers. Along with the rotating wafer, a non-rotating TC-wafer with seven thermocouples attached on the upper side of wafer surface has also been employed for the research. Fig. 2 illustrates the arrangement of the TH lamp array and the location of the temperature sensors. During wafer heating, nitrogen is supplied at 15 SLM (standard liter per minute). In practical operation for production wafers, it is normally required that the absolute temperature control error over the wafer surface is less than 1 °C.

MODEL IDENTIFICATION

1. Model Linearization and Sampling Period

Basically, RTP systems are highly nonlinear because of complicated radiation dominant heat transfer. For precise tracking control in such systems, a linearization method valid over a wide range needs to be introduced unless nonlinear model-based control is attempted. Under the assumption that both wafer surface and chamber wall are gray, diffuse, and opaque, Cho et al. [8] have shown that the relationship between the fourth power of the wafer temperature and the lamp power is linear (more precisely, affine) under a steady state. They have extended the relationship to linear dynamic modeling and could have attained a superior performance to the case where the wafer temperature itself is taken as the output of a linear dynamic model.

In this research, we followed Cho et al.'s approach [8], i.e., represented the RTP system as a linear dynamic model with u_j's and T_i^4's as input and output variables, where u_j and T_i denote the lamp power (in percent) of the j^{th} circle and the i^{th} pyro-temperature in Kelvin, respectively. Preliminary step tests showed that the time constants are in the range of 20 to 40 sec. However, to effectively cope with potential problems related to high rate ramping and short processing time, the sampling period was chosen to be 0.5 sec throughout the study.

2. Identification Experiments

The wafer temperature was steered to a prescribed steady state by four separate PID controllers that manipulate the powers of lamp circles grouped into four. After reaching the steady state, the controllers were switched to the manual state and input excitation was started under the open-loop. One lamp circle was perturbed at a time for three minutes according to a pre-designed PRBS (pseudo-random binary sequence) from circle one to ten for sequential SIMO identification. The minimum switching time of the PRBS was extended such that the band width of the signal spectrum conformed roughly to that of the RTP system, which was estimated from the step test responses.

Separate identifications were done for the rotating wafer and the non-rotating TC-wafer, respectively, both at around 880 °C.

3. Estimation of MIMO State Space Model

SIMO identification is in fact equivalent to multiple independent SISO identifications. Since the concerned RTP system has ten inputs and four outputs, 40 SISO models were found separately from the

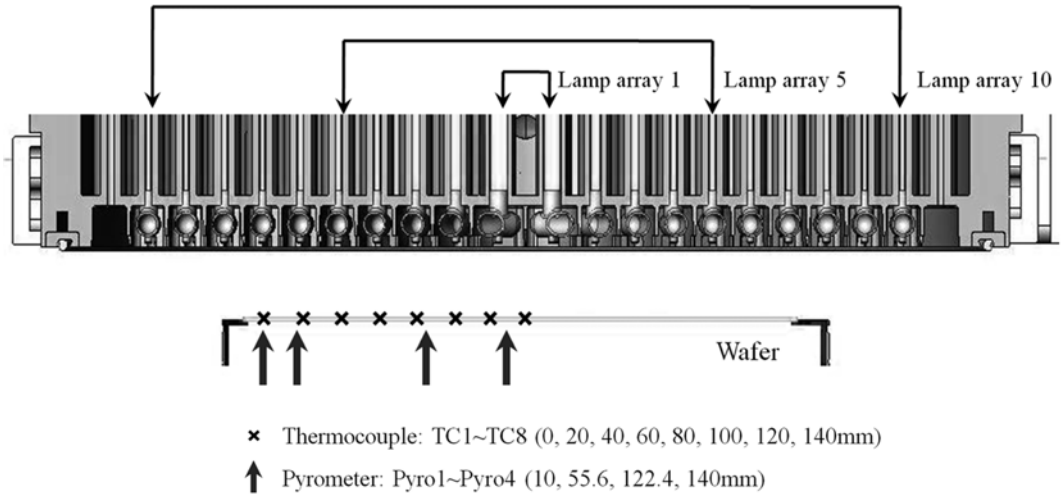

Fig. 2. Tungsten-halogen lamp array and temperature sensor locations.

experimental data. Each of them was realized as a canonical form and then combined to form an augmented state space model, which was finally reduced to a minimal state space model through balanced truncation. Details of each step are as follows:

• Step 1: Each SISO map is identified as a high-order ARX model. A high-order ARX model is advantageous over other model structures in that the linear least squares method can be used for parameter estimation and unbiased estimates are obtained even under correlated noises [12]. For de-trending, the model was found between the time difference signals as follows:

$$\begin{aligned}&\Delta y(t)+a_1\Delta y(t-1)+\cdots+a_n\Delta y(t-n)=b_1\Delta u(t-1)+\cdots+b_n\Delta u(t-n)+e(t)\\&\quad\Leftrightarrow A(q^{-1})\Delta y(t)=B(q^{-1})\Delta u(t)+e(t)\end{aligned}\tag{1}$$

where $\Delta u(t)\triangleq u(t)-u(t-1)$, $\Delta y(t)\triangleq y(t)-y(t-1)$, and e(t) represents a zero-mean residual signal, respectively. Here, u(t) refers to a lamp circle power in percent and y(t) represents the scaled $T^4[K^4]$, i.e., $y(t)\triangleq T^4(t)/\alpha$ for some α.

• Step 2: The ARX model is converted to a canonical state space model (controllable form in this study). Let the associated system matrices be $(a_{m,n}, b_{m,n}, c_{m,n})$ where $_{m,n}$ indicates the model between the n^{th} input and the m^{th} output.

• Step 3: The state space models are combined to constitute an augmented model. For the 4×10 model case, it was represented as

$$\begin{aligned}\bar{x}(t+1)&=\begin{bmatrix}a_{1,1}&\cdots&0&\cdots&0&\cdots&0\\\vdots&\ddots&\vdots&\ddots&\vdots&\ddots&\vdots\\0&\cdots&a_{1,10}&\ddots&0&\cdots&0\\\vdots&\ddots&\ddots&\ddots&\ddots&\ddots&\vdots\\0&\cdots&0&\ddots&a_{4,1}&\cdots&0\\\vdots&\ddots&\vdots&\ddots&\vdots&\ddots&\vdots\\0&\cdots&0&\cdots&0&\cdots&a_{4,10}\end{bmatrix}\bar{x}(t)\\&\quad+\begin{bmatrix}b_{1,1}&\cdots&0\\\vdots&\ddots&\vdots\\0&\cdots&b_{1,10}\\\vdots&\ddots&\vdots\\b_{4,1}&\cdots&0\\\vdots&\ddots&\vdots\\0&\cdots&b_{4,10}\end{bmatrix}\Delta U(t)\\&\triangleq\bar{A}\bar{x}(t)+\bar{B}\Delta U(t)\end{aligned}\tag{2}$$

$$\begin{aligned}\Delta Y(t)&=\begin{bmatrix}c_{1,1}&\cdots&c_{1,10}&\cdots&0&\cdots&0\\0&\cdots&0&\ddots&0&\cdots&0\\0&\cdots&0&\cdots&c_{4,1}&\cdots&c_{4,10}\end{bmatrix}\bar{x}(t)\\&\triangleq\bar{C}\bar{x}(t)\end{aligned}$$

where

$$\begin{aligned}&\bar{x}(t)\triangleq[x_{1,1}(t)^T\ x_{1,2}(t)^T\ \cdots\ x_{4,10}(t)^T]^T,\\&\Delta Y(t)\triangleq[\Delta y_1(t)\ \cdots\ \Delta y_4(t)]^T,\\&\Delta U(t)\triangleq[\Delta u_1(t)\ \cdots\ \Delta u_{10}(t)]^T\end{aligned}\tag{3}$$

• Step 4: The model in Eq. (2) is non-minimal. Hence reduction is necessary to obtain a minimal realization. For this, balanced truncation is applied to $(\bar{A}, \bar{B}, \bar{C})$. The resulting reduced model is defined as $(\hat{A}, \hat{B}, \hat{C})$ [13,14].

• Step 5: The state space model is rearranged to have ΔU(t) and Y(t) as the input and output variables for the integral action to be included in the controller as follows:

$$\begin{aligned}\begin{bmatrix}\hat{x}(t+1)\\Y(t)\end{bmatrix}&=\begin{bmatrix}\hat{A}&0\\\hat{C}&I\end{bmatrix}\begin{bmatrix}\hat{x}(t)\\Y(t-1)\end{bmatrix}+\begin{bmatrix}\hat{B}\\0\end{bmatrix}\Delta U(t)\\Y(t)&=[\hat{C}\ \ I]\begin{bmatrix}\hat{x}(t)\\Y(t-1)\end{bmatrix}\end{aligned}\tag{4}$$

which is redefined as

$$\begin{aligned}x(t+1)&=Ax(t)+B\Delta U(t)\\Y(t)&=Cx(t)\end{aligned}\tag{5}$$

For the TC-wafer, a steady state gain matrix between the lamp powers and seven TC-temperatures in scaled $T^4[K^4]$ was determined for R2R control from a separate state space model identified up to step 4 in addition to a dynamic model between the lamp powers and pyro-temperatures for LQG control.

CONTROLLER DESIGN

LQG control was employed for MIMO control of the pyro-temperatures. However, MIMO control alone is not enough to assure the temperature uniformity since the four pyrometer measurements cannot represent the temperature distribution over the entire wafer surface. For this, R2R control was designed to adjust the extra degree of input freedom for uniformity improvement and LQG control was modified to accommodate the command signals from the R2R controller.

1. Real-time LQG Control

The standard LQG tracking objective was modified to admit the input bias values from the R2R controller as follows:

$$\begin{aligned}\min_{\Delta U(\cdot)}\frac{1}{2}\Big[&\|\bar{r}(N)-Cx(N)\|^2_{\bar{M}}\\&+\sum_{t=0}^{N-1}\{\|\bar{r}(t)-Cx(t)\|^2_{\bar{Q}(t)}+\|\Delta U(t)\|^2_{\bar{R}(t)}+\|U(t-1)-U_b\|^2_{\bar{S}(t)}\}\Big]\end{aligned}\tag{6}$$

where $\|x\|^2_P\triangleq x^TPx$; $\bar{r}(t)$ denotes the reference temperature trajectory; $\|U(t-1)-U_b\|^2_{\bar{S}(t)}$ is to push U(t−1) to U_b, which is provided by R2R control.

To convert the above to the standard LQG objective, we augment the state by including U(t), which is an integral of ΔU(t), and transform the state space equation in Eq. (5) as follows:

$$\begin{aligned}\begin{bmatrix}x(t+1)\\U(t)\end{bmatrix}&=\begin{bmatrix}A&0\\0&I\end{bmatrix}\begin{bmatrix}x(t)\\U(t-1)\end{bmatrix}+\begin{bmatrix}B\\I\end{bmatrix}\Delta U(t)\\\begin{bmatrix}Y(t)\\U(t-1)\end{bmatrix}&=\begin{bmatrix}C&0\\0&I\end{bmatrix}\begin{bmatrix}x(t)\\U(t-1)\end{bmatrix}\end{aligned}\tag{7}$$

which is redefined as

$$\begin{aligned}z(t+1)&=\Phi z(t)+\Gamma\Delta U(t)\\\begin{bmatrix}Y(t)\\U(t-1)\end{bmatrix}&=\Sigma z(t)\end{aligned}\tag{8}$$

Accordingly, the LQG objective in Eq. (6) can be written with

the new state variable as

$$\min_{\Delta U(\cdot)} \frac{1}{2}\left[\|r(N) - \Sigma z(N)\|_M^2 + \sum_{t=0}^{N-1} \{\|r(t) - \Sigma z(t)\|_{Q(t)}^2 + \|\Delta U(t)\|_{R(t)}^2\} \right] \quad (9)$$

where $r(t) \triangleq [\bar{r}(t)^T \; U_b^T]^T$, $M \triangleq \mathrm{diag}[\overline{M}, \overline{S}(N)]$, and $Q(t) \triangleq \mathrm{diag}[\overline{Q}, \overline{S}(t)]$, respectively. The above is a standard LQG tracking problem and the solution is given as follows [15]:

$$\Delta U(t) = K_{fb}(t) z(t) + K_{ff}(t) b(t+1) \quad (10)$$

where

$$\begin{aligned} K_{fb}(t) &= -(R + \Gamma^T P(t+1) \Gamma)^{-1} \Gamma^T P(t+1) \Phi \\ K_{ff}(t) &= (R + \Gamma^T P(t+1) \Gamma)^{-1} \Gamma^T \\ P(t) &= \Phi^T P(t+1) \Phi - \Phi^T P(t+1) \Gamma (R + \Gamma^T P(t+1) \Gamma)^{-1} \Gamma^T P(t+1) \Phi \\ &\quad + \Sigma^T Q(t+1) \Sigma, \; P(N) = \Sigma^T M \Sigma \\ P(t) &= -\Phi^T P(t+1)(I - \Gamma (R + \Gamma^T P(t+1) \Gamma)^{-1} \Gamma^T P(t+1)) \Gamma R^{-1} \Gamma^T b(t+1) \\ &\quad + \Phi^T b(t+1) + \Sigma^T Q(t+1) r(t), \; b(N) = \Sigma^T M r(N) \end{aligned} \quad (11)$$

In real implementation, z(t) is replaced by an estimate z(t|t) which can be obtained by the Kalman filter constructed on Eq. (8) [15].

The reference temperature trajectory consists of ramping and dwell periods and $\overline{S}(t)$ was set to be zero for the ramping period and to increase gradually over the dwell period in order to prevent U_b from drawing U(t) too strongly when the system undergoes dynamics.

2. Run-to-run Control

The role of R2R control is to enhance the temperature uniformity by manipulating U_b through run-wise feedback of OT or RS measurements. In this study, TC-temperatures replaced the OT or RS measurements.

Let Ψ be the steady state TC measurements (in K^4) in the dwell period and the steady state map between U_b and Ψ be represented by

$$\Psi = KU_b + \Psi_b \quad (12)$$

where Ψ_b denotes a bias term including a run-independent random part. Let Υ be the target value of Ψ and define $E \triangleq \Upsilon - \Psi$. Also let

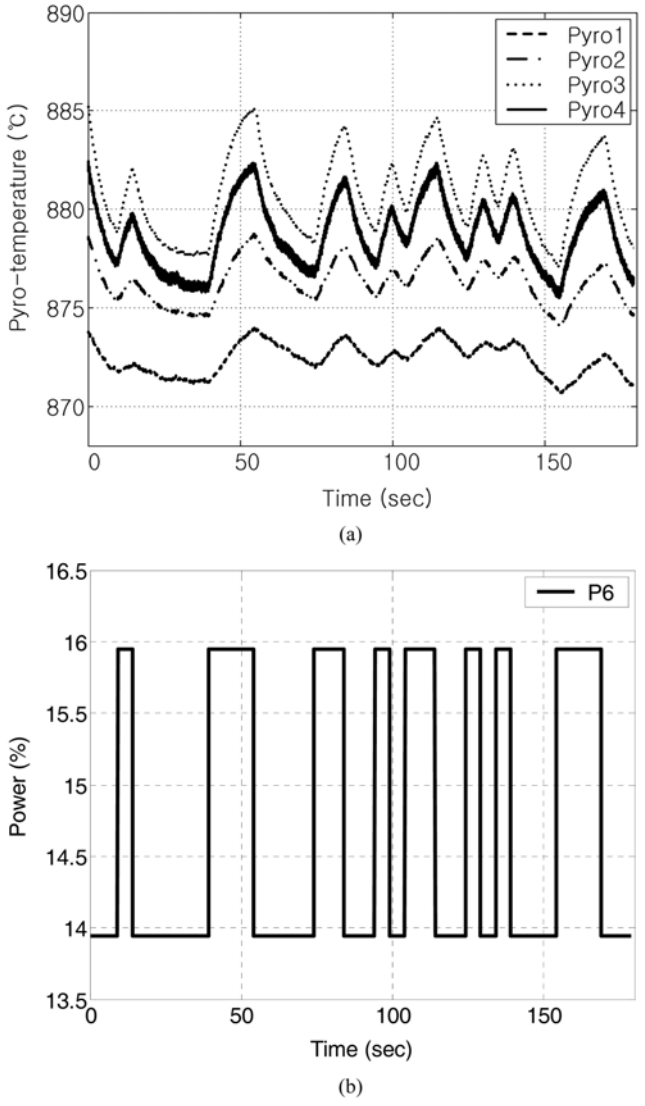

Fig. 3. Pyro-temperatures trajectories for changes in sixth lamp group around 880 °C; (a) pyro-temperatures, (b) Input excitation signal (PRBS).

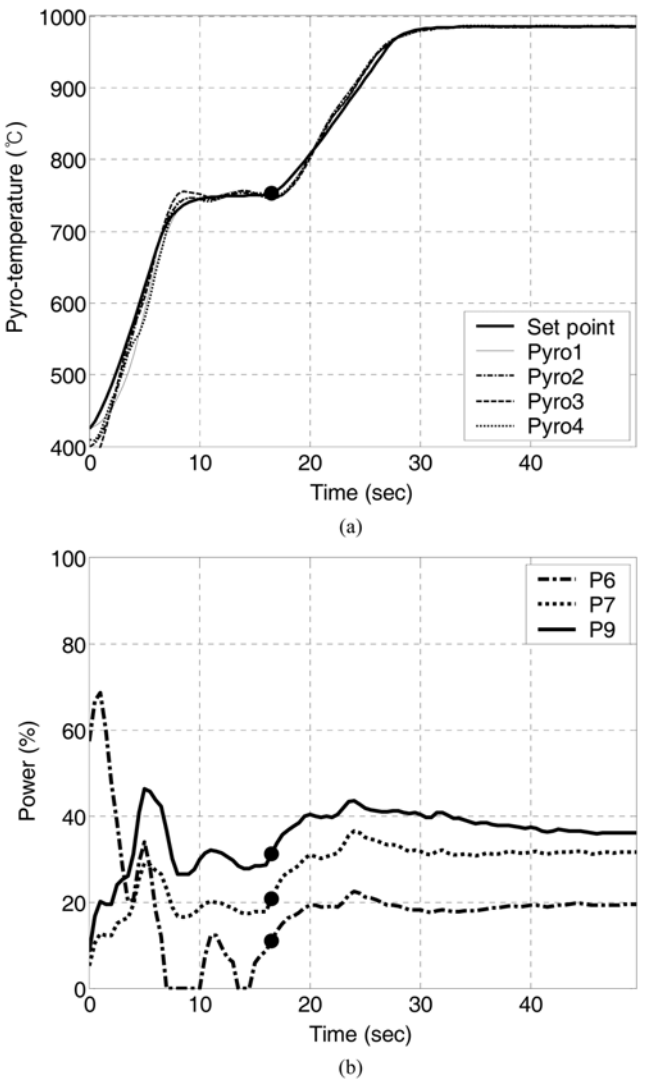

Fig. 4. Results of LQG tracking with wafer rotation - dwell temperature of 985 °C; (a) pyro-temperatures, (b) input profiles.

the subscript $_k$ represent the run index. If we subtract both sides of Eq. (12) from Υ, write the resulting equations for $_{k+1}$ and $_k$, and take the difference between them, we can derive the following run-wise error update equation:

$$E_{k+1}=E_k-K\Delta U_{b,k+1}+n_{k+1} \tag{13}$$

where $\Delta U_{b,k+1}\triangleq U_{b,k+1}-U_{b,k}$; $n_{k+1}\triangleq \Psi_{b,k+1}-\Psi_{b,k}$ represents a zero-mean run-wise random vector. $\Delta U_{b,k+1}$ can be determined after each run according to the QILC law [16] such that the one-run-ahead prediction of output error is minimized.

$$\min_{\Delta U_{b,k+1}} J(\Delta U_b)=\frac{1}{2}\{\|E_{k+1|k}\|_\Lambda^2+\|\Delta U_{b,k+1}\|_\Omega^2\} \tag{14}$$

subject to $0\le U_{b,k+1}\le 100$

where $E_{k+1|k}=E_k-K\Delta U_{b,k+1}$. For the unconstrained case, $\Delta U_{b,k+1}$ is given as

$$\Delta U_{b,k+1}=(K^T\Lambda K+\Omega)^{-1}K^T\Lambda E_k \tag{15}$$

After the k^{th} run, $U_{b,k+1}=U_{b,k}+\Delta U_{b,k+1}$ is sent to the LQG controller for the $k+1^{th}$ run.

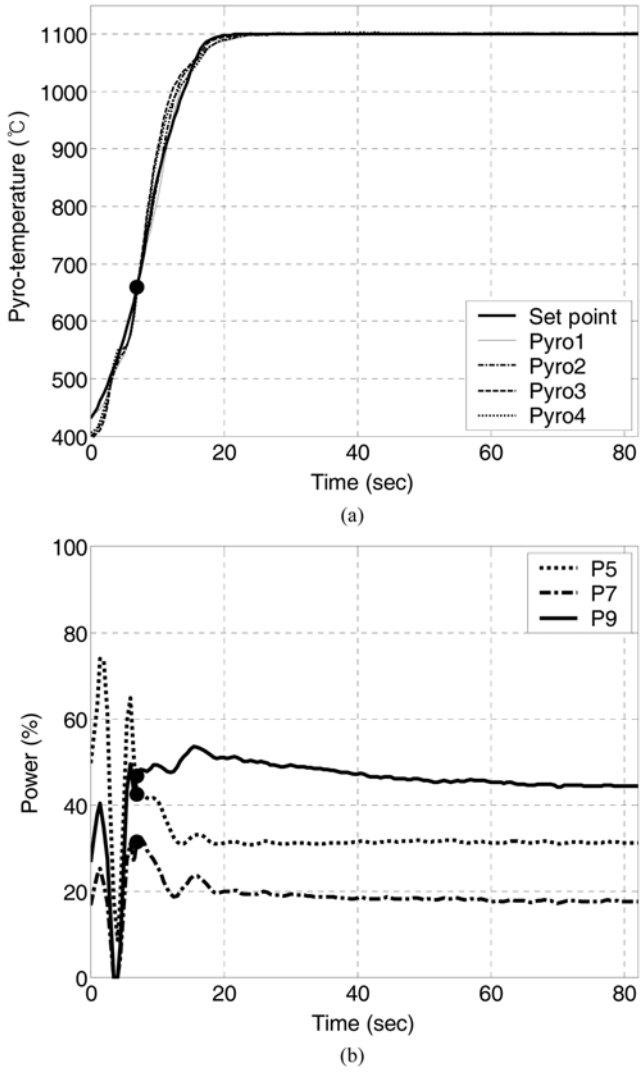

Fig. 5. Results of LQG tracking with wafer rotation - dwell temperature of 1,100°C; (a) pyro-temperatures, (b) input profiles.

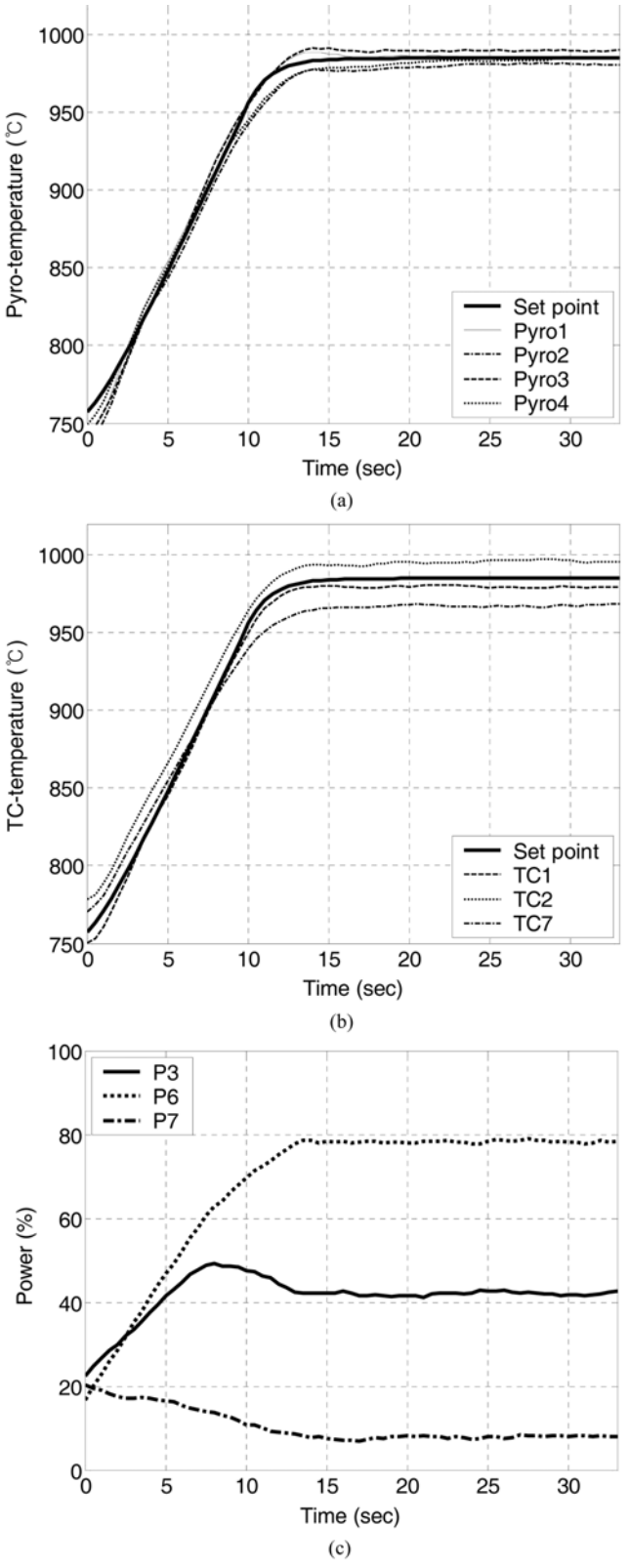

Fig. 6. Closed-loop responses under LQG control before R2R control is put into action; (a) pyro-temperatures, (b) TC-temperatures, (c) input profiles.

RESULTS AND DISCUSSION

Fig. 3 shows a typical response of selected pyro-temperatures to a PRBS excitation in a lamp circle power. The order of the ARX model was determined parsimoniously by auditing the whiteness of the residual term and it was found that 10 to 13 was most appropriate depending on input-output pairs. The dimension of the state $\hat{x}$ after the balanced truncation was determined to be 85.

Fig. 4(a) shows a result of LQG tracking of pyro-temperatures with wafer rotation. The reference trajectory is composed of ramping-up from 400 °C at 50 °C/sec followed by 10 sec of hold at 750 °C, ramping-up again at 25 °C/sec and dwelling at 985 °C for 20 sec. For the initial period until the moment marked by a filled circle where the second ramping starts, only the Kalman filter was in action under PID control. From then on, LQG control was executed. One can see that nice tracking as well as quite accurate regulation could be achieved. The regulation error during the last 15 sec in the dwell period was less than 1.0 °C. Fig. 4(b) exhibits the corresponding input responses for three selected lamp circles. Fig. 5 shows a result similar to Fig. 4 but for a different trajectory with ramping rate of 35 °C/sec and dwell temperature of 1,100 °C. LQG control began from 660 °C after the Kalman filter was run under PID control. The regulation error during the last 25 sec in the dwell period was kept less than 0.8 °C in this case. For both cases, the input bias penalty was not considered by setting $\overline{S}(t)=0$.

It is worth noting that LQG control was designed with a model identified at 880 °C, but performs nicely for the higher temperature trajectories. This verifies the model can appropriately represent the system over a wide temperature range.

The performance of combined R2R and LQG control for the non-rotating TC-wafer is summarized in Figs. 6 to 8. For the concerned RTP system, the control performance is worsened when the wafer rotation is turned off. Under this condition, the maximum difference between pyro-temperatures is easily widened to 8 °C or more under feedback control. To avoid complexity in display, three (maximum, minimum, and middle) out of the seven TC-temperatures and also three out of ten lamp powers are selected and plotted in all figures. First, Fig. 6 exhibits the initial LQG performance before R2R control is put into action. The input bias penalty was not activated. It can be seen that the pyro-temperatures show a relatively good

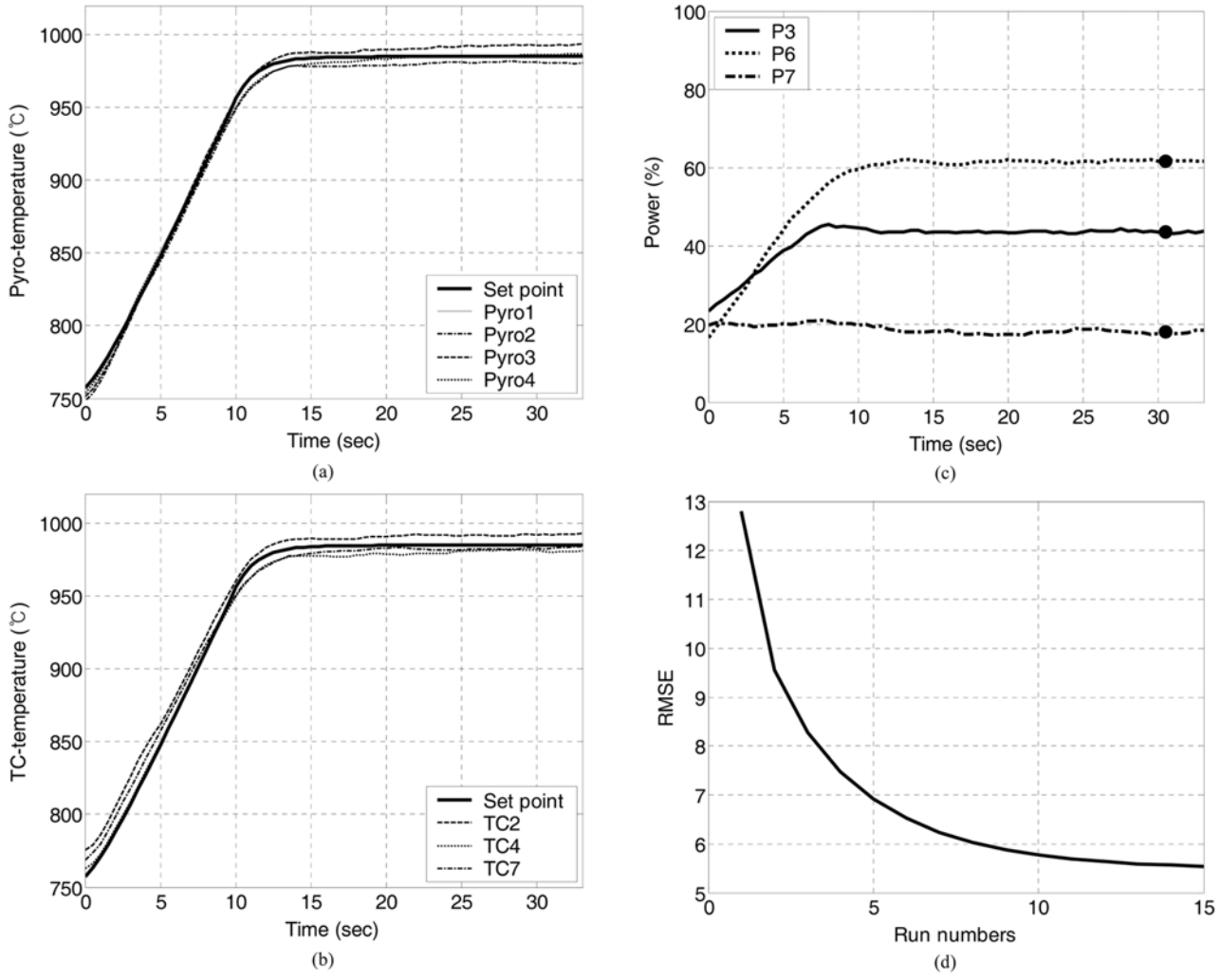

Fig. 7. Closed-loop responses under LQG control after 15 consecutive runs - U_b is updated over the whole space of the steady state map between U and Y; (a) pyro-temperatures, (b) TC-temperatures, (c) input profiles, (d) root mean squared error.

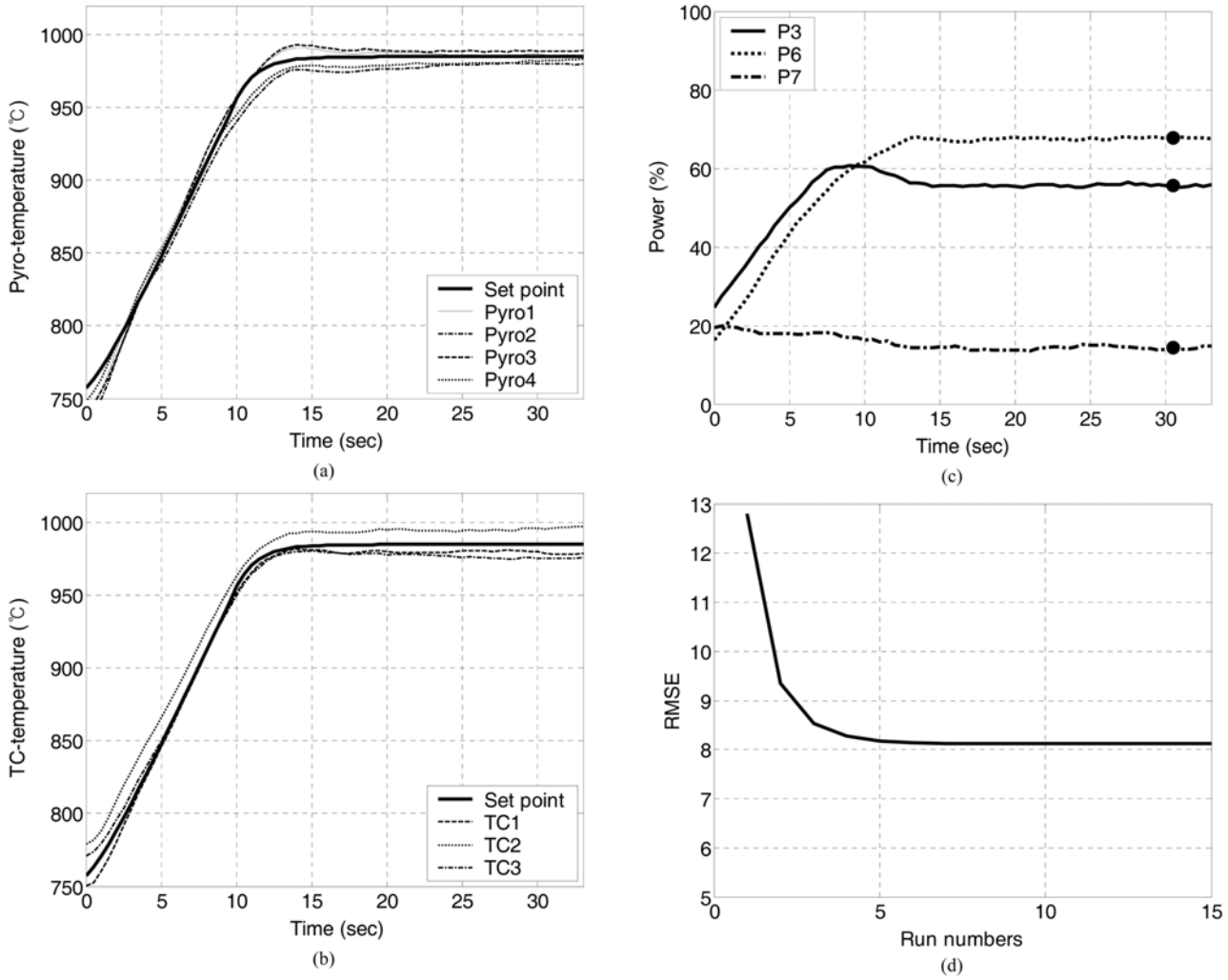

Fig. 8. Closed-loop responses under LQG control after 15 consecutive runs - U_b is updated only over the null space of the steady state map between U and Y; (a) pyro-temperatures, (b) TC-temperatures, (c) input profiles, (d) root mean squared error.

tracking performance (for the case of non-rotating wafer) whereas the TC-temperatures produce the maximum temperature difference of about 30 ºC. Starting from the initial run, R2R control updates U_b to reduce the regulation error of the TC-temperatures. Fig. 7 summarizes the results after 15 consecutive runs. It can be seen that TC-temperature profiles are narrowed closely around the target value with the maximum temperature difference reduced to 12.4 ºC. On the other hand, the regulation performance of the pyro-temperatures was sacrificed a little bit with the temperature difference being widened to 13 ºC from 9 ºC. By comparing Figs. 6(c) and 7(c), one can see that the selected lamp power trajectories changed quite a great deal under R2R control. Fig. 7(d) exhibits how the root mean squared error (RMSE) of the steady state TC-temperatures defined as RMSE $=\sqrt{(1/7)\Sigma_{i=1}^{7}(T_i-T_{sp})^2}$, where T_{sp} represents the set point, was decreased with the run number under R2R control.

In addition to the proposed R2R control, we also attempted a modified R2R scheme that updates U_b only over the null space of the steady state map between U and Y (fourth power of pyro-temperatures) such that

$$U_{b,k}=U_{ss}+V_N\theta_k \quad (16)$$

where U_{ss} and V_N represent a steady state input and a basis of the null space, respectively. The idea behind this method is to adjust only the extra degree of input freedom while not sacrificing the LQG performance. R2R control calculates θ_k which updates U_b indirectly. Fig. 8 summarizes the experimental results after 15 runs. It can be observed that the LQG performance was kept almost intact as shown in Fig. 8(a). On the other hand, the maximum TC-temperature difference was reduced only to 23 ºC, which is almost twice of the difference in Fig. 7(b), and consequently the RMSE was decreased not as much as in Fig. 7(d).

CONCLUSIONS

A combined R2R and LQG control method has been devised and applied to a 12-inch RTP equipment for run-to-run improvement together with real-time control of wafer temperature uniformity. R2R control has been designed to update the steady state powers of the tungsten-halogen lamp groups so that the uniformity of post-batch measurements like oxide layer thickness or resistivity over the wafer surface can be improved. LQG control performs real-time tracking of pyrometer temperatures. The standard LQG cost was

modified to accommodate the input bias provided by the R2R controller. The MIMO state space model for the controller design was determined through balanced truncation of a non-minimal MIMO realization of multiple high-order SISO ARX models, which were estimated by using the data obtained from sequential SIMO identification experiments. To construct a linear time-invariant model valid over a wide range of temperatures, the model output was defined as the fourth power of the wafer temperature (in K).

Experiments were conducted in 12-inch commercial RTP equipment where four pyrometers are installed. Test of LQG control was conducted with a normal wafer under wafer rotation and regulation error of less than 1 ºC could have been attained for dwell temperatures of 985 ºC and 1,100 ºC, respectively. The combined R2R and LQG control method has been investigated with a non-rotating TC-wafer that has seven TC attachments in addition to four pyrometers. With the TC-temperatures as replacement of RTO or RS measurements, it was found that the proposed method functions satisfactorily as expected, improving the temperature uniformity as the run number increases.

Further research is still under way to search for methods to shorten the sampling time not incurring numerical problems for the case of higher ramping rates and to cut the required computation, which is burdensome with the present embedded DSP (digital signal processor) controller.

ACKNOWLEDGMENTS

The authors would like to acknowledge the financial support from the KORNIC Systems Co., Ltd. W. Won also would like to acknowledge the financial support from the Seoul Metropolitan Government.

REFERENCES

1. T. F. Edgar, S. W. Butler, W. J. Campbell, C. Pfeiffer, C. Bode and S. B. Hwang, *Automatica*, **36**(11), 1567 (2000).
2. K. S. Balakrishnan and T. F. Edgar, *Thin Solid Films*, **365**, 322 (2000).
3. C. J. Huang, C. C. Yu and S. H. Shen, *Automatica*, **36**(5), 705 (2000).
4. K. S. Lee, J. Lee I. S. Chin, J. Choi and J. H. Lee, *Ind. Eng. Chem. Res*., **40**(7), 1661 (2001).
5. D. R. Yang, K. S. Lee and H. J. Ahn, *IEEE Trans. Semicond. Manufact*., **16**(1), 36 (2003).
6. W. Cho, PhD Dissertation, University of Texas at Austin (2005).
7. M. Cho, S. Joo, S. Won and K. S. Lee, *Can. J. Chem. Eng*., **83**, 371 (2005).
8. M. Cho, Y. Lee, S. Joo and K. S. Lee, *IEEE Trans. Semicond. Manufact*., **18**(3), 430 (2005).
9. J. Y. Choi, H. M. Do and H. S. Choi, *IEEE Trans. Semicond. Manufact*., **16**(4), 621 (2003).
10. C. D. Schaper, T. Kailath and Y. J. Lee, *IEEE Trans. Semicond. Manufact*., **12**(2), 193 (1999).
11. Y. M. Cho and P. J. Gyugyi, *IEEE Trans. Contr. Syst. Technol*., **5**(6), 644 (1997).
12. L. Ljung, *System identification: Theory for the user*, Prentice Hall, New Jersey (1999).
13. M. G. Safonov and R. Y. Chiang, *IEEE Trans. Automatic Cont*., **34**(7), 729 (1989).
14. C. T. Chen, *Linear system theory and design*, Oxford, New York (1999).
15. F. L. Lewis and V. L. Syrmos, *Optimal control*, John Wiley and Sons, New York (1995).
16. J. H. Lee, K. S. Lee and W. C. Kim, *Automatica*, **36**(5), 641 (2000).